

Generic conditions for stable hybrid stars

Mark G. Alford, Sophia Han (韩君)

Physics Department, Washington University, St. Louis, MO 63130, USA

Madappa Prakash

Department of Physics and Astronomy, Ohio University, Athens, OH 45701, USA

(Dated: 15 May 2013)

We study the mass-radius curve of hybrid stars, assuming a single first-order phase transition between nuclear and quark matter, with a sharp interface between the quark matter core and nuclear matter mantle. We use a generic “classical ideal gas” (CIG) parameterization of the quark matter equation of state, which has a density-independent speed of sound. We argue that this parameterization provides a general framework for comparison and empirical testing of models of quark matter. We obtain the phase diagram of possible forms of the hybrid star mass-radius relation, where the control parameters are the transition pressure, energy density discontinuity, and the quark matter speed of sound. We find that this diagram is sensitive to the quark matter parameters but fairly insensitive to details of the nuclear matter equation of state.

We calculate the maximum hybrid star mass as a function of the parameters of the quark matter EoS, and find that there are reasonable values of those parameters that give rise to hybrid stars with mass above $2 M_{\odot}$.

PACS numbers: 25.75.Nq, 26.60.-c, 97.60.Jd,

I. INTRODUCTION

There has been much work on a plausible form for the equation of state (EoS) of nuclear matter at densities above nuclear density, using models of the nuclear force that are constrained by existing scattering data (see, for example, [1–3]). However, we remain almost completely ignorant of the quark matter EoS at the low temperatures and the range of densities that are of relevance to neutron stars. This is because cold quark matter cannot be created in laboratories, and numerical studies using the known strong interaction Lagrangian are stymied by the sign problem (see, for example, [4–7]).

In this work we therefore assume a generic quark matter equation of state, and see in what ways it might be constrained by measurements of the mass and radii of compact stars. We assume that there is a first-order phase transition between nuclear and quark matter, and that the surface tension of the interface is high enough to ensure that the transition occurs at a sharp interface (Maxwell construction) not via a mixed phase (Gibbs construction). This is a possible scenario, given the uncertainties in the value of the surface tension [8–10]. (For analysis of generic equations of state that continuously interpolate between the phases to model mixing or percolation, see Refs. [11, 12].)

It is already known [13–15] that there is a simple criterion, in terms of the discontinuity in the energy density at the transition, that specifies when hybrid stars with an arbitrarily small core (i.e. with central pressure just above the transition) will be stable. In this paper we look at the properties of the hybrid star branch from the transition up to higher central pressures, assuming that the quark matter EoS has a density-independent speed of sound like a classical ideal gas (“CIG”)[36]. We obtain

the phase diagram of the possible forms of the hybrid star branches, and find that it is fairly insensitive to details of the nuclear matter equation of state. We also investigate the observability of the hybrid star branches, and the maximum mass as a function of the parameters of the quark matter EoS.

To address these questions we parameterize the quark matter EoS in terms of three quantities: the pressure p_{trans} of the transition from nuclear matter to quark matter, the discontinuity in energy density $\Delta\epsilon$ at the transition, and the speed of sound c_{QM} in the CIG parameterization of quark matter, which we assume remains constant as the pressure varies from p_{trans} up to the central pressure of the maximum mass star. The equation of state for dense matter is therefore approximated as (see Fig. 1)

$$\epsilon(p) = \begin{cases} \epsilon_{\text{NM}}(p) & p < p_{\text{trans}} \\ \epsilon_{\text{NM}}(p_{\text{trans}}) + \Delta\epsilon + c_{\text{QM}}^{-2}(p - p_{\text{trans}}) & p > p_{\text{trans}} \end{cases} \quad (1)$$

where $\epsilon_{\text{NM}}(p)$ is the nuclear matter equation of state. In Appendix A we describe the thermodynamically consistent parameterization of the EoS that we used for quark matter. A similar generic parameterization was proposed in Ref. [16], which also considered the possibility of two first-order transitions involving two different phases of quark matter.

• Quark Matter EoS.

The assumption that quark matter behaves like a Classical Ideal Gas with a density-independent speed of sound is reasonably consistent with some well-known quark matter equations of state. For some Nambu–Jona-Lasinio models, the CIG EoS fits Eq. (1) almost exactly [16]. In addition, the perturbative quark matter EoS [17] has roughly density-independent c_{QM}^2 , with a value around 0.2 to 0.3, above the transition from nuclear mat-

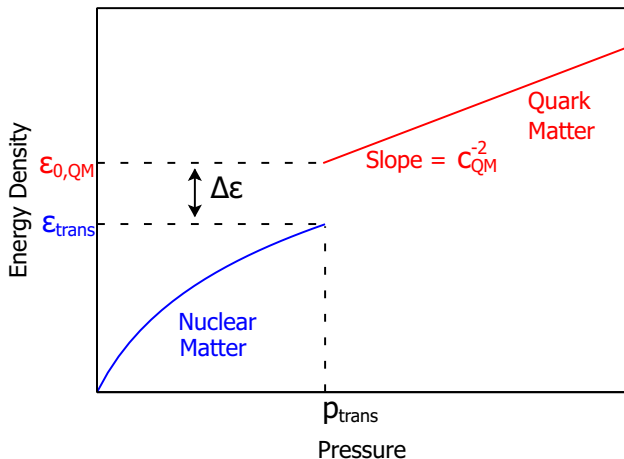


FIG. 1: Equation of state $\varepsilon(p)$ for dense matter. The quark matter EoS is specified by the transition pressure p_{trans} , the energy density discontinuity $\Delta\varepsilon$, and the speed of sound in quark matter c_{QM} (assumed density-independent).

EoS	max mass	radius at $M = 1.4 M_{\odot}$	L
NL3	$2.77 M_{\odot}$	14.92 km	118 MeV
HLPS	$2.15 M_{\odot}$	10.88 km	33 MeV

TABLE I: Properties of the NL3 and HLPS equations of state. L characterizes the density-dependence of the symmetry energy (see text). NL3 is an example of a stiff EoS, HLPS is an example of a softer one at density $n \lesssim 4n_0$.

ter (see Fig. 9 of Ref. [18]). In the quartic polynomial parameterization [19], varying the coefficient a_2 between $\pm(150\text{MeV})^2$, and the coefficient a_4 between 0.6 and 1, and keeping n_{trans}/n_0 above 1.5 ($n_0 \equiv 0.16\text{fm}^{-3}$ is the nuclear saturation density), one finds that c_{QM}^2 is always between 0.3 and 0.36.

In this paper we study hybrid stars for a range of values of c_{QM}^2 , from $1/3$ (characteristic of very weakly interacting massless quarks) to 1 (the maximum value consistent with causality). We expect that this will give us a reasonable idea of the likely range of outcomes for realistic quark matter.

- **Nuclear Matter EoS.** Up to densities around nuclear saturation density n_0 , the nuclear matter EoS can be experimentally constrained. If one wants to extrapolate it to densities above n_0 , there are many proposals in the literature. For illustrative purposes, we use two examples: a relativistic mean field model labelled NL3 [20] and a non-relativistic potential model labelled HLPS, corresponding to “EoS1” in Ref. [2]. Since HLPS is only defined at $n > 0.5n_0$, we continued it to lower density by switching to NL3 for $n < 0.5n_0$. Some of the properties of HLPS and NL3 are summarized in Table I, where L is related to the derivative of the symmetry energy S_2 with respect to density at the nuclear saturation density, $L = 3n_0(\partial S_2/\partial n)|_{n_0}$.

HLPS is a softer equation of state, with a lower value

of L and lower pressure at a given energy density (up to $p \approx 3 \times 10^9 \text{ MeV}^4$, $n \approx 5.5n_0$ where its speed of sound rises above 1 and becomes unphysical). NL3 is a stiffer EoS, with higher pressure at a given energy density (also, its speed of sound is less than 1 at all pressures). It yields neutron stars that are larger, and can reach a higher maximum mass.

There is some evidence favoring a soft EoS for nuclear matter: in Ref. [21], values in the range $L = 40$ to 60 MeV were favored from an analysis of constraints imposed by available laboratory and neutron star data. Using data from X-ray bursts, Ref. [22] finds the surface to volume symmetry energy ratio $S_s/S_v \approx 1.5 \pm 0.3$ (See after their Eq. (43) and Table 4), which corresponds to L in the range $22 \pm 4 \text{ MeV}$ (using Eq. (7) in Ref. [21]).

- **Nuclear/Quark transition.** The nuclear matter to quark matter transition occurs at pressure p_{trans} . We will sometimes specify its position in terms of the energy density $\varepsilon_{\text{trans}}$ of nuclear matter at the transition, or the ratio $p_{\text{trans}}/\varepsilon_{\text{trans}}$. Since the nuclear matter EoS has $d^2\varepsilon/dp^2 < 0$ at high densities (Fig. 1), p/ε increases monotonically with p , ε , and n , so it is a proxy for the transition pressure or density.

- **Organization of paper.** In Sec. II we discuss the criteria for stable hybrid stars to exist, as a function of the nuclear matter equation of state and the parameters of our generic quark matter equation of state. Sec. III presents the phase diagram for hybrid star branches as a function of the parameters of the CIG EoS for quark matter. In Sec. IV we discuss the maximum mass that such hybrid stars can achieve. Sec. V gives a summary and conclusions.

II. CRITERION FOR STABLE HYBRID STARS

A. Connected hybrid branch

A compact star will be stable as long as the mass M of the star is an increasing function of the central pressure p_{cent} [23]. There will therefore be a stable hybrid star branch in the $M(R)$ relation, connected to the neutron star branch, if the mass of the star continues to increase with p_{cent} when the quark matter core first appears, at $p_{\text{cent}} = p_{\text{trans}}$. When the quark matter core is sufficiently small, its effect on the star, and hence the existence of a connected hybrid star branch, is determined entirely by the energy density discontinuity $\Delta\varepsilon$ at its surface, since the quark core is not large enough for the slope (c_{QM}^{-2}) of $\varepsilon(p)$ to have much influence on the mass and radius of the hybrid star. This fact was pointed out in Ref. [13] where the dependence on $\Delta\varepsilon$ was expressed in terms of the parameter $q \equiv 1 + \Delta\varepsilon/\varepsilon_{\text{trans}}$. A more detailed treatment in Ref. [14, 24] used a parameter λ with the same definition, and calculated the linear response to a small quark matter core in terms of λ . Ref. [15] used the parameter $\Delta \equiv \Delta\varepsilon/(\varepsilon_{\text{trans}} + p_{\text{trans}})$ and highlighted the occurrence of a cusp in the $M(R)$ relation (see below).

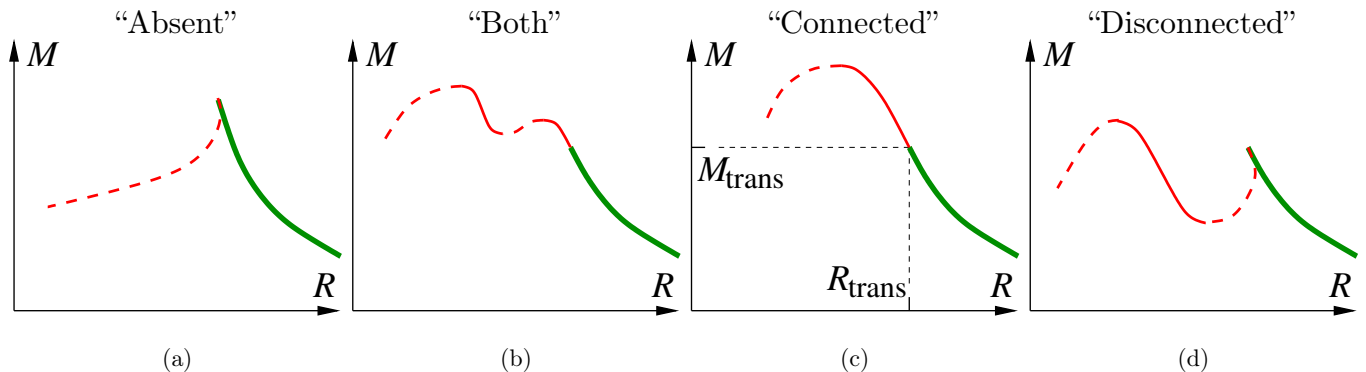


FIG. 2: Schematic form of possible mass-radius relations for hybrid stars. The thick (green) line is the hadronic branch. Thin solid (red) lines are stable hybrid stars; thin dashed (red) lines are unstable hybrid stars. In (a) the hybrid branch is absent. In (c) there is a connected branch. In (d) there is a disconnected branch. In realistic neutron star $M(R)$ curves the cusp that occurs in cases (a) and (d) is much smaller and harder to see [14, 15]

If $\Delta\varepsilon$ is small then quark matter has a similar energy density to that of nuclear matter, and we expect a connected hybrid branch that looks roughly like a continuation of the nuclear matter branch. If $\Delta\varepsilon$ is too large, then the star becomes unstable as soon as the quark matter core appears, because the pressure of the quark matter is unable to counteract the additional downward force from the gravitational attraction that the additional energy in the core exerts on the rest of the star. By performing an expansion in powers of the size of the quark matter core, one can show [13–15] that there is a stable hybrid star branch connected to the neutron star branch if $\Delta\varepsilon$ is less than a threshold value $\Delta\varepsilon_{\text{crit}}$ given by

$$\frac{\Delta\varepsilon_{\text{crit}}}{\varepsilon_{\text{trans}}} = \frac{1}{2} + \frac{3}{2} \frac{p_{\text{trans}}}{\varepsilon_{\text{trans}}}. \quad (2)$$

(This is $\lambda_{\text{crit}} - 1$ in the notation of Ref. [14].) As $\Delta\varepsilon$ approaches the threshold value $\Delta\varepsilon_{\text{crit}}$ from below, both dM/dp_{cent} and dR/dp_{cent} approach zero linearly as $p - p_{\text{cent}}$, with the result that the slope dM/dR of the mass radius curve is independent of $\Delta\varepsilon$. For $\Delta\varepsilon < \Delta\varepsilon_{\text{crit}}$, the hybrid star branch continues with the same slope as the neutron star mass-radius relation at the transition to quark matter. When $\Delta\varepsilon$ exceeds $\Delta\varepsilon_{\text{crit}}$, dM/dR is unchanged, but flips around so that there is a cusp when the central pressure reaches p_{trans} [15], at $(M, R) = (M_{\text{trans}}, R_{\text{trans}})$. This is shown in schematic form in Fig. 2, where panels (b) and (c) show possible forms of $M(R)$ for $\Delta\varepsilon < \Delta\varepsilon_{\text{crit}}$, and panels (a) and (d) show possible forms for $\Delta\varepsilon > \Delta\varepsilon_{\text{crit}}$. In $M(R)$ curves for realistic neutron star equations of state, the cusp at high $\Delta\varepsilon$ is much less clearly visible: the region where the slopes of hybrid and neutron stars match is very small, covering a range in M of less than one part in a thousand near the transition point $(R_{\text{trans}}, M_{\text{trans}})$ [15].

B. Disconnected hybrid branch

In Figs. 2(b) and (d), we illustrate the occurrence of a second, disconnected, branch of stable hybrid stars at $\Delta\varepsilon > \Delta\varepsilon_{\text{crit}}$. This possibility was noted in Ref. [14]. The disconnected branch is a “third family” [25, 26] of compact stars besides neutron stars and white dwarfs. Third families have been found in $M(R)$ calculations for specific quark matter models, for example kaon condensed stars [27], quark matter cores from perturbative QCD [28], and color superconducting quark matter cores [29]. In this paper we will study the generic features of a quark matter EoS that give rise to this phenomenon. In principle one could imagine that additional disconnected stable branches might occur, but we do not find any with the ideal-gas-type quark matter EoS that we use in this paper.

III. “PHASE DIAGRAM” FOR HYBRID STARS

A. Phase diagram at fixed c_{QM}

In Fig. 3 we plot a “phase diagram” for hybrid stars, where the control parameters are two of the parameters of the CIG quark matter EoS: $p_{\text{trans}}/\varepsilon_{\text{trans}}$ (the ratio of pressure to energy density in nuclear matter at the transition pressure) and $\Delta\varepsilon$ (the discontinuity in the energy density at the transition). The quark matter speed of sound is held constant. As noted in Sec. I, $p_{\text{trans}}/\varepsilon_{\text{trans}}$ increases monotonically with pressure, so it is a proxy for the transition pressure or density. Our phase diagram covers a range in $p_{\text{trans}}/\varepsilon_{\text{trans}}$ from 0.02 up to about 0.5. Below 0.02 the NL3 EoS has a baryon density far below n_0 , and the HLPs EoS has a discontinuity in c^2 that is not physical.

The left panel of Fig. 3 is the result of calculations for the HLPs nuclear matter EoS and quark matter with $c_{\text{QM}}^2 = 1$. The lower x-axis shows $p_{\text{trans}}/\varepsilon_{\text{trans}}$, which is

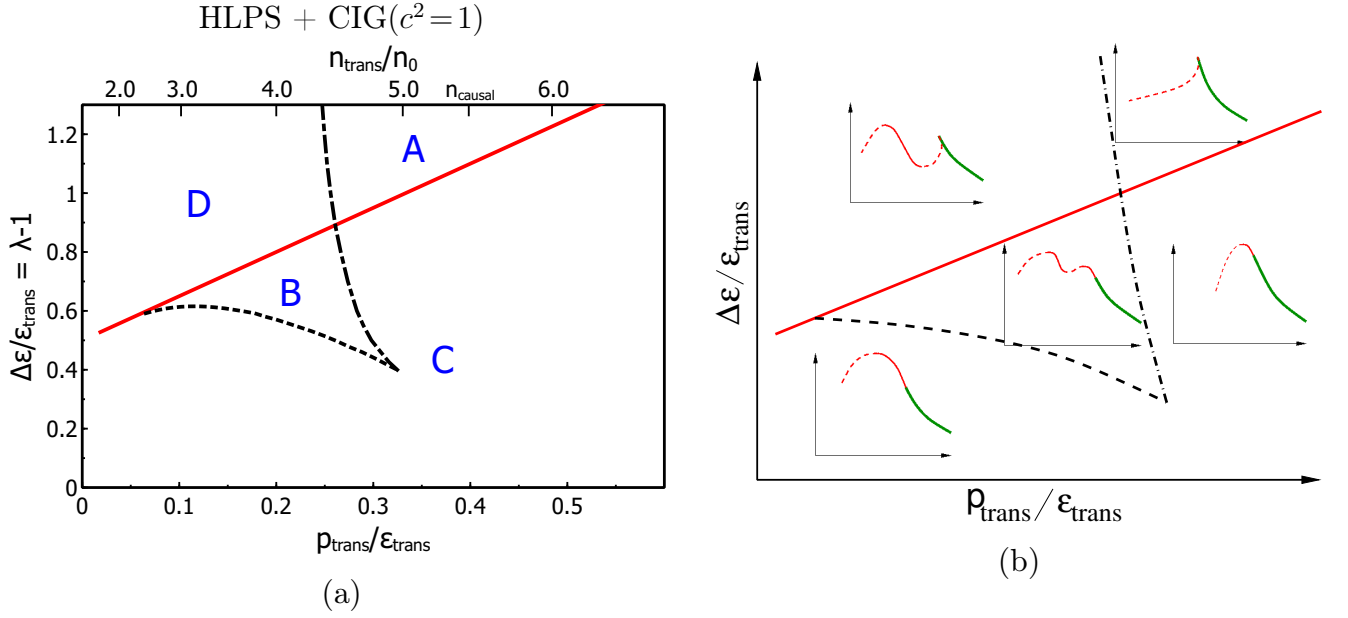


FIG. 3: Phase diagram for hybrid star branches in the mass-radius relation of compact stars. The control parameters are the pressure p_{trans} and energy density discontinuity $\Delta\epsilon$ at the transition, each expressed in units of the nuclear energy density at the transition ϵ_{trans} . The y-axis is therefore just a shifted version of the parameter λ of Ref. [14]. The solid straight line is $\Delta\epsilon_{\text{crit}}$ (Eq. (2)). The left panel is the result of calculations for a softer nuclear matter EoS (HLPS) and Classical Ideal Gas (CIG) quark matter with $c_{\text{QM}}^2 = 1$. The right panel is a schematic showing the form of the mass-radius relation in each region of the diagram: regions A,B,C,D correspond to Fig. 2(a),(b),(c),(d).

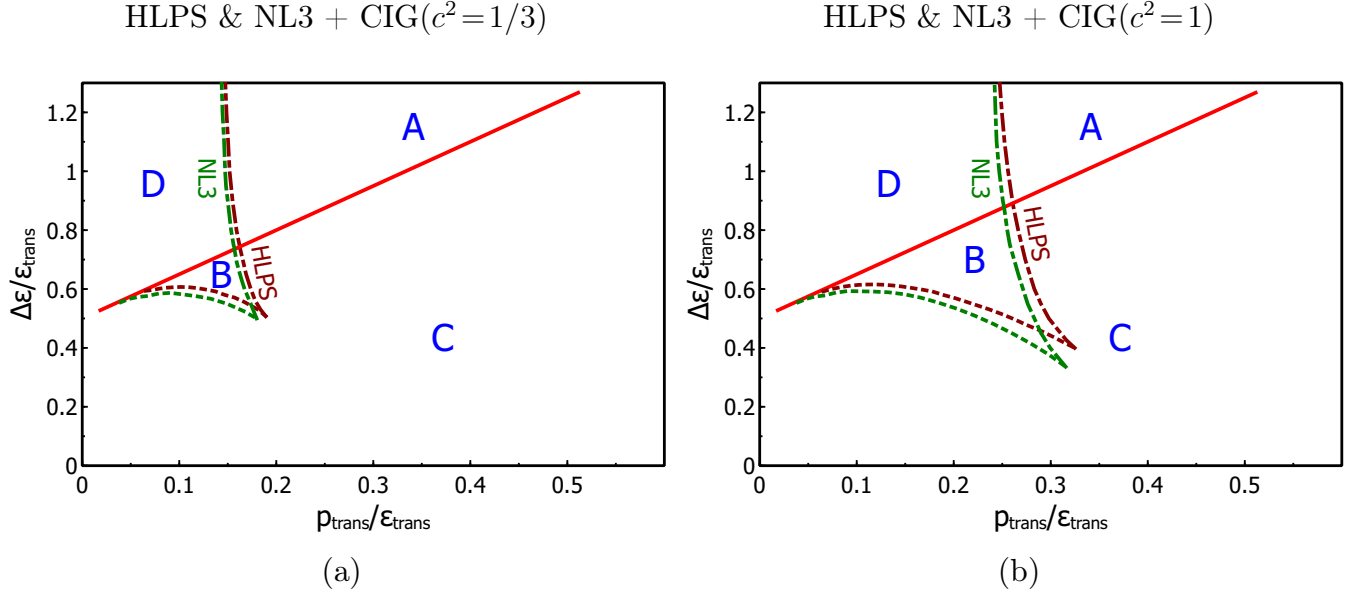


FIG. 4: Phase diagram like Fig. 3, showing that the phase boundaries are not very sensitive to changes in the nuclear matter EoS, but they are affected by varying the quark matter speed of sound.

the natural way to characterize the transition. The upper x-axis shows the corresponding transition baryon density of nuclear matter for the HLPS EoS. HLPS becomes acausal at $n = 5.458 n_0$, but all the interesting structure in the plot is below this density. The right panel is a schematic showing the form of the mass-radius relation in each region of the diagram. The regions correspond

to different geometries of the hybrid branch displayed in Fig. 2: A=“Absent”, C=“Connected”, D=“Disconnected”, B=“Both” (connected and disconnected).

The solid straight (red) line is $\Delta\epsilon_{\text{crit}}$ from Eq. (2). On crossing this line $M'(p_{\text{cent}})$ and $R'(p_{\text{cent}})$ both change sign when quark matter first appears, causing the $M(R)$ curve to undergo a discontinuous change, flipping around

from being “upward-pointing” (mass increases with central pressure) and continuous, to being “downward-pointing” (mass decreases with central pressure) with a cusp. Below the line ($\Delta\varepsilon < \Delta\varepsilon_{\text{crit}}$), in regions B and C, there is a hybrid star branch connected to the nuclear star branch. Above the line ($\Delta\varepsilon > \Delta\varepsilon_{\text{crit}}$), in regions A and D, there is no connected hybrid star branch. In regions B and D there is a disconnected hybrid star branch.

The roughly vertical dash-dotted curve in Fig. 3 marks a transition where an additional disconnected branch of hybrid stars appears/disappears. When one crosses this line from the right, going from region A to D by decreasing the nuclear/quark transition density, a stationary point of inflection appears in $M(p_{\text{cent}})$ at $p_{\text{cent}} > p_{\text{trans}}$. If one crosses from C to B then this point of inflection is at lower central pressure than the existing maximum in $M(p_{\text{cent}})$. This produces a stationary point of inflection in the $M(R)$ relation to the left of the existing maximum (if any). After crossing the dash-dotted line the point of inflection becomes a new maximum-minimum pair (the maximum being further from the transition point), producing a disconnected branch of stable hybrid stars in regions B and D. Crossing the other way, by increasing the transition pressure, the maximum and minimum that delimit the disconnected branch merge and the branch disappears.

The roughly horizontal dashed curve in Fig. 3 which separates region B and C marks a transition between mass-radius relations with one connected hybrid star branch, and those with two hybrid star branches, one connected and one disconnected. Crossing this line from below, by increasing the energy density discontinuity, a stationary point of inflection in $M(p_{\text{cent}})$ (or equivalently in $M(R)$) appears in the existing connected hybrid branch. Crossing in to region B, this point of inflection becomes a new maximum-minimum pair, so the connected hybrid branch is broken in to a smaller connected branch and a new disconnected branch. The maximum of the old connected branch smoothly becomes the maximum of the new disconnected branch. If one crossed the dashed line in the opposite direction, from B to C, the maximum closest to the transition point would approach the minimum and they would annihilate, leaving only the more distant maximum.

Where the horizontal and vertical curves meet, the two maxima and the minimum that are present in region B all merge to form a single flat maximum where the first three derivatives of $M(R)$ are all zero.

Along the critical line Eq. (2), which is the straight line in Fig. 3, $dM/dp_{\text{cent}} = 0$ at $p_{\text{cent}} = p_{\text{trans}}$. We now discuss the curvature $M'' \equiv d^2M/dp_{\text{cent}}^2$ at $p_{\text{cent}} = p_{\text{trans}}$ on that line. On the A/C boundary, $M'' < 0$. In region C there is a maximum in $M(p_{\text{cent}})$ at $p_{\text{cent}} > p_{\text{trans}}$, but on the A/C boundary that maximum has shifted to $p_{\text{cent}} = p_{\text{trans}}$. As we move down the A/C boundary, M'' becomes less negative. This continues along the B/D boundary, until at the point where the B/C boundary (dashed line) merges with the B/D boundary,

$M'' = 0$. This is because the stationary point of inflection in $M(p_{\text{cent}})$ (where the disconnected branch first appears) has now arrived at $p_{\text{cent}} = p_{\text{trans}}$. Continuing down the critical line, M'' becomes positive, making it possible for there to be a direct transition between C and D.

B. Varying c_{QM} and the nuclear EoS

Up to now we have discussed the effects of varying two of the parameters of the quark matter EoS, namely p_{trans} and $\Delta\varepsilon$. In Fig. 4 we show the effects of varying the third parameter, the speed of sound, and the effect of varying the nuclear matter EoS. Fig. 4(a) is the phase diagram for CIG quark matter with $c_{\text{QM}}^2 = 1/3$, and Fig. 4(b) is for $c_{\text{QM}}^2 = 1$. In both panels we show the phase diagram for a softer (HLPS) nuclear matter EoS and a harder (NL3) nuclear matter EoS. As expected from Eq. (2) the straight line where the connected hybrid branch disappears is independent of c_{QM}^2 and the detailed form of the nuclear matter EoS. The other phase boundaries, outlining the region where there is a disconnected hybrid branch, are remarkably insensitive to the details of the nuclear matter EoS. However, they depend strongly on the quark matter speed of sound. For a given nuclear matter EoS the hybrid branch structure is determined by $p_{\text{trans}}/\varepsilon_{\text{trans}}$, $\Delta\varepsilon/\varepsilon_{\text{trans}}$, and c_{QM}^2 , so one could make a three-dimensional plot with c_{QM}^2 as the third axis, but this figure adequately illustrates the dependence on c_{QM}^2 . We will now discuss the physics behind the shape of the phase boundaries.

C. Physical understanding of the phase diagram

The main feature of the phase diagram is that a disconnected branch is present when the transition density is sufficiently low, and the energy density discontinuity is sufficiently high, namely in regions B and D. It occurs more readily (i.e. those regions are larger) if the speed of sound in quark matter is high. Such features were noticed in the context of stars with mixed phases in Ref. [11], which pointed out that they can be understood as follows.

When a very small quark matter core is present, its greater density creates an additional gravitational pull on the nuclear mantle. If the pressure of the core can counteract the extra pull, the star is stable and there is a connected hybrid branch (regions C and B). If the energy density jump is too great, the extra gravitational pull is too strong, and the star becomes unstable when quark matter first appears (regions A and D). However, if the energy density of the core rises slowly enough with increasing pressure (i.e. if $c^2 = dp/d\varepsilon$ is large enough), a larger core with a higher central pressure may be able to sustain the weight of the nuclear mantle above it (region

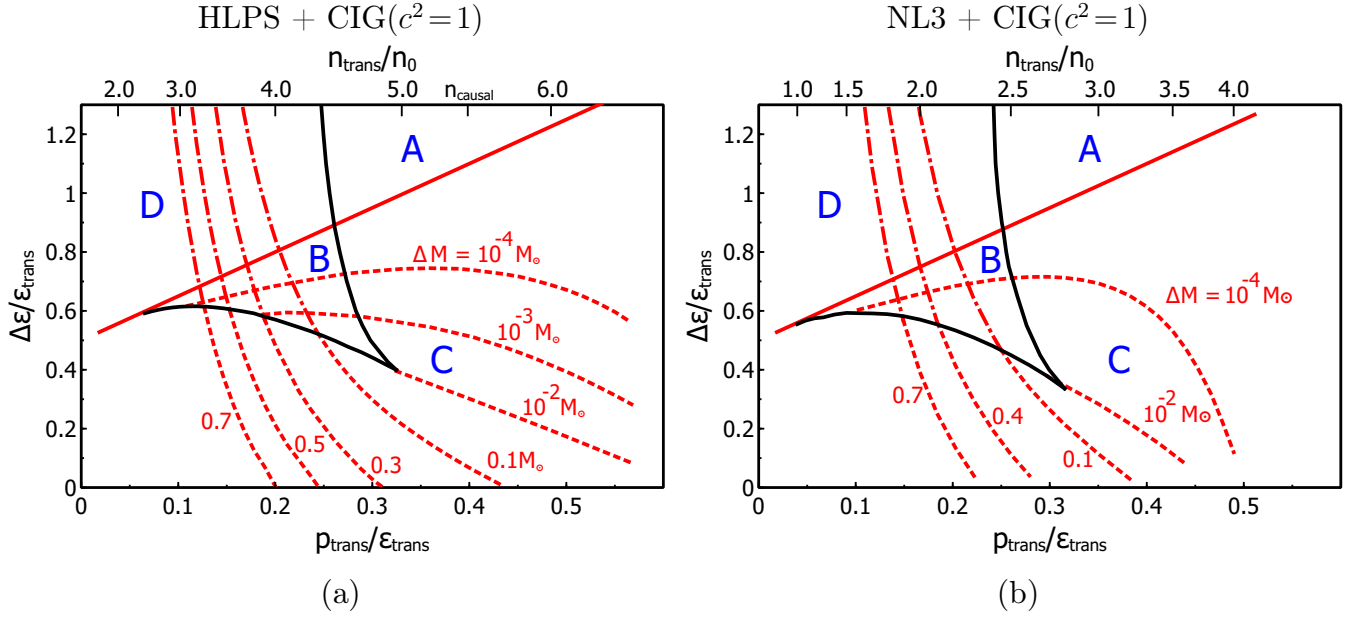


FIG. 5: Contour plot of a measure of the observability of hybrid branches: ΔM , the mass difference between the heaviest hybrid star and the hadronic star when quark matter first appears. We show results for HLPS and NL3 nuclear matter, with $c_{\text{QM}}^2 = 1$ CIG quark matter. The contours are not very sensitive to details of the nuclear matter EoS. If the transition density is high, or if a disconnected branch is present, the connected branch may be very small and hard to observe.

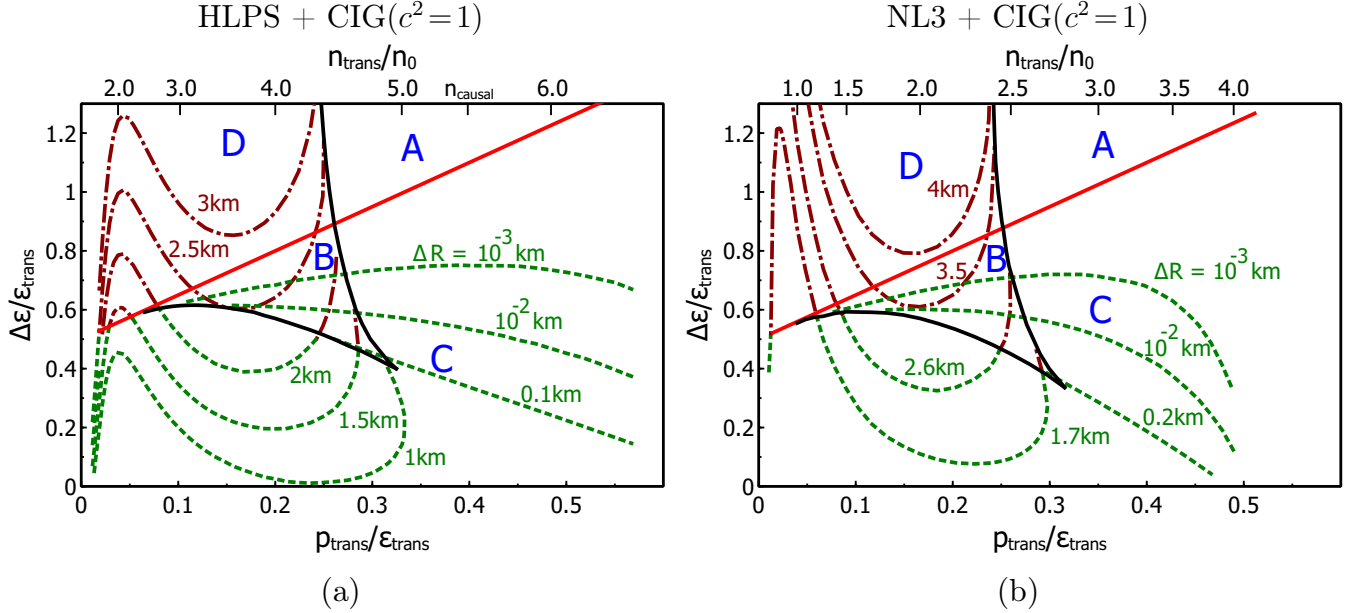


FIG. 6: Contour plot of a measure of the observability of hybrid branches: ΔR , the difference between the radius of the hadronic star when quark matter first appears and the radius of the heaviest hybrid star. We show results for HLPS and NL3 nuclear matter, with $c_{\text{QM}}^2 = 1$ CIG quark matter. The contours are not very sensitive to details of the nuclear matter EoS. If the transition density is high, or if a disconnected branch is present, the connected branch may be very small and hard to observe.

D). Region B, with connected and disconnected branches, is more complicated and we do not have an intuitive explanation for it.

We can now understand why the vertical line marking the B/C and D/A boundaries moves to the right as c_{QM}^2 increases. Since $c^2 = dp/d\epsilon$, if c_{QM}^2 is larger then

the energy density of the core rises more slowly with increasing pressure, which minimizes the tendency for a large core to destabilize the star via its gravitational attraction. Finally, we can see why that line has a slight negative slope: larger $\Delta\epsilon$ makes the quark core heavier, increasing its pull on the nuclear mantle, and making the

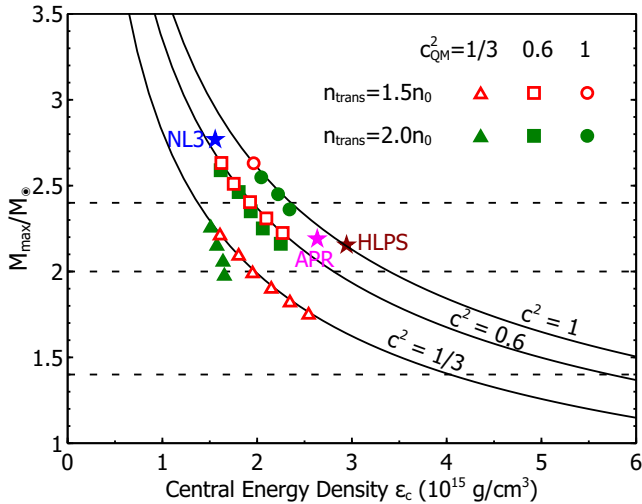


FIG. 7: Mass of the heaviest hybrid star as a function of its central energy density, for various quark matter equations of state (1). The curves are predictions of Ref. [30] for stars whose core-region speed of sound squared is 1, 0.6, and 1/3. Pure nuclear matter stars for the NL3 and APR equations of state are also plotted.

hybrid star more unstable against collapse.

Ref. [11], assuming a mixed phase, conjectured that the third family (disconnected branch) exists when the speed of sound in quark matter is higher than that in the mixed phase. However, our results do not support that conjecture. In the case we study, with no mixed phase, the relevant quantity would be the difference between c_{QM} (the speed of sound in quark matter) and c_{NM} (the speed of sound in nuclear matter at the phase transition). If the conjecture were correct, our phase diagram (which is for fixed c_{QM}) would show the disconnected branch appearing at a vertical phase boundary located at the transition pressure where $c_{NM} = c_{QM}$. In fact, as seen in Fig. 4, we find one horizontal phase boundary, and a near-vertical boundary. For $c_{QM}^2 = 1$ quark matter the vertical boundary occurs at $p_{\text{trans}}/\varepsilon_{\text{trans}} \approx 0.3$ where $c_{NM}^2 \approx 0.75$ for HLPS and $c_{NM}^2 \approx 0.65$ for NL3. For $c_{QM}^2 = 1/3$ quark matter the vertical boundary occurs at $p_{\text{trans}}/\varepsilon_{\text{trans}} \approx 0.15$ where $c_{NM}^2 \approx 0.5$ for HLPS and NL3. We conclude that the appearance of a disconnected branch is not determined by whether $c_{QM} > c_{NM}$.

D. Observability of hybrid branches

The phase diagrams of the previous subsection show us when connected and disconnected branches are present, but for astrophysical observations it is important to know how easily these branches could be detected via measurements of the mass and radius of compact stars. In Figs. 5 and 6 we show the phase diagram for HLPS and NL3 nuclear matter, with $c_{QM}^2 = 1$ quark matter, with contours

showing two measures, ΔM and ΔR , of the length of the hybrid branch. ΔM is the difference in mass between the heaviest hybrid star and the hadronic star just before quark matter appears (whose mass is M_{trans}). ΔR is the difference in radius between the hadronic star just before quark matter appears (whose radius is R_{trans}) and the heaviest hybrid star. At the horizontal boundary between region C and B, the maximum of the connected branch smoothly becomes the maximum of the disconnected branch (see Fig. 3) so the dashed contours (for the connected branch) connect smoothly to the dot-dashed contours (for the disconnected branch). We see that the ΔM and ΔR contours are roughly independent of details of the nuclear matter EoS, except at high transition pressure where the transition to quark matter is happening close to the maximum of the nuclear EoS, which greatly suppresses the length of the connected branch. Note that although we only show contours for positive ΔM and ΔR , contours that end on the A/D or near-vertical B/C boundary can have negative ΔM .

From Figs. 5 and 6 we conclude that Eq. (2) is not a good guide to the presence of *observable* hybrid branches. The connected branch may be very small and hard to detect, even at values of $\Delta\varepsilon/\varepsilon_{\text{trans}}$ well below the critical value of Eq. (2). For the $c_{QM}^2 = 1$ case, only in the parts of region C that lie approximately below region B (i.e. for $p_{\text{trans}}/\varepsilon_{\text{trans}} \lesssim 0.3$) is the connected hybrid branch large enough to be detectable via observations of mass that have an experimental uncertainty of around $0.01M_{\odot}$ or observations of radius that have an uncertainty of around 0.2 km. When a disconnected branch is present, the connected branch is either absent (region D) or too small to observe (region B).

The disconnected branch itself, whose presence has nothing to do with Eq. (2), is in principle easily observable except perhaps at the far right edge of regions B and D. The natural way for the disconnected branch to be populated would be via accretion, taking a star to the top of the connected branch, after which it would have to collapse to the disconnected branch, with dramatic emission of neutrinos and gamma rays [31] and gravitational waves [32]. It is not clear how one would populate the parts of the disconnected branch that lie below that mass threshold, so one might end up with a gap in the observed radii of neutron stars, where the populated sequence jumps from one branch to the other.

IV. MAXIMUM MASS OF HYBRID STARS

A. Maximum mass and central energy density

The CIG quark matter EoS (1) involves three parameters, p_{trans} (or equivalently n_{trans}), $\Delta\varepsilon$, and c_{QM} . The results of Ref. [30, 33] lead us to expect that, for a given nuclear matter EoS, the maximum mass M_{max} is mostly determined by the central energy density of the heaviest star and the speed of sound in the central regions of that

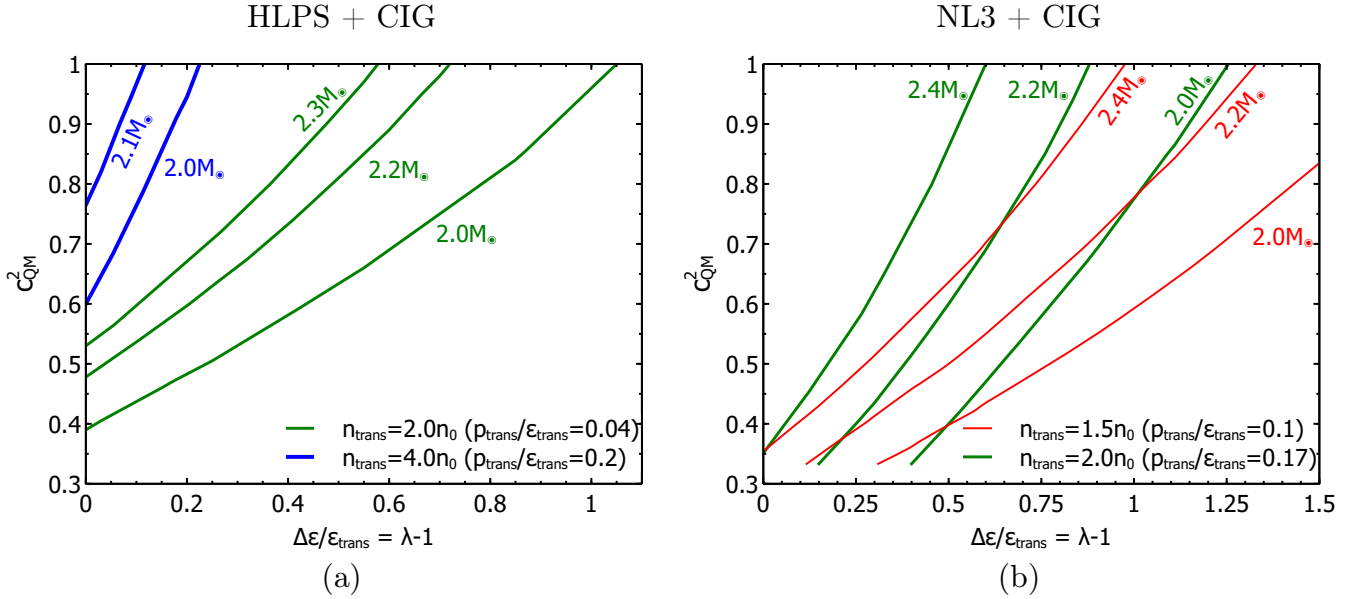


FIG. 8: Contour plot of the mass of the heaviest hybrid star as a function of quark matter EoS parameters $p_{\text{trans}}/\epsilon_{\text{trans}}$, c_{QM}^2 , and $\Delta\epsilon/\epsilon_{\text{trans}}$ (a shifted version of λ in Ref. [14]) for HLPS and NL3 nuclear matter. The thin (red), medium (green) and thick (blue) lines are for a nuclear to quark transition at $n_{\text{trans}} = 1.5n_0$, $2n_0$, and $4n_0$, respectively.

star. Specifically,

$$M_{\text{max}} \stackrel{?}{=} y(c_{\text{cent}}) \epsilon_{\text{cent}}^{-1/2}. \quad (3)$$

The function $y(c_{\text{cent}})$ can be obtained from Ref. [30] (their Eq. (24) and the associated table). To test Eq. (3), we follow Ref. [30, 33] and plot the maximum mass M_{max} that a stable star can have, as a function of the central energy density in that star ϵ_{cent} . We use the NL3 nuclear matter EoS and repeat the calculation for a range of quark matter equations of state, varying the transition density n_{trans} for the transition to quark matter, the quark matter speed of sound c_{QM} , and the energy density discontinuity $\Delta\epsilon$ at the transition. The range of allowed values of $\Delta\epsilon$, giving stable hybrid stars is from zero to $\Delta\epsilon_{\text{crit}}(n_{\text{trans}})$.

The results are shown in Fig. 7, where we use the NL3 nuclear matter EoS and CIG Quark Matter. The solid curves show $M_{\text{max}}(\epsilon_{\text{cent}})$ according to Eq. (3) for $c_{\text{cent}}^2 = 1, 0.6$, and $1/3$. Nuclear matter equations of state at high density have c^2 close to 1, hence the maximum masses for pure nuclear matter stars (we show the result for APR [1] nuclear matter as well as NL3 and HLPS) lie close to the $c_{\text{cent}}^2 = 1$ line.

The triangles, squares, and circles show the masses of hybrid stars for a quark matter EoS with relatively low transition densities: $n_{\text{trans}} = 1.5n_0$ (open symbols) or $n_{\text{trans}} = 2n_0$ (solid symbols), and for each of these we vary c_{QM} and $\Delta\epsilon$. The low transition density means that these hybrid stars have large quark matter cores, so the the speed of sound in the central part of the star is c_{QM} , so the maximum masses should fall on the lines given by Eq. (3) with $c_{\text{cent}} = c_{\text{QM}}$. We see that on the whole this is the case. However, for $n_{\text{trans}} = 2.0n_0$ and $c_{\text{QM}}^2 = 1/3$

(solid triangles) the points fall slightly below the predicted $c_{\text{QM}}^2 = 1/3$ line. This implies that in these stars the effective speed of sound in the core is even lower than $1/\sqrt{3}$. However, the speed of sound in the NL3 nuclear matter mantle at $n \sim 2n_0$ is greater than $1/\sqrt{3}$. It seems reasonable to argue that the first-order phase transition, at which $dp/d\epsilon = c^2$ vanishes, acts like a “soft” region where c is small [16], and drags down the average value of c_{cent} . All hybrid stars have such a transition region, but in these stars the quark matter cores are smaller than in the other cases, so the nuclear-quark matter boundary is closer to the center of the star, and by the conjecture of Ref. [33] it is expected to play a more important role in determining the maximum mass.

B. How heavy can a hybrid star be?

Using the CIG parameterization (1) of the quark matter EoS, it is possible to get hybrid stars that are heavy enough to be consistent with recent measurements of stars of mass $2M_{\odot}$ [34, 35]. In Fig. 8 we show contour plots for the maximum masses of hybrid stars as a function of the parameters of the quark matter EoS, for both the HLPS and NL3 nuclear equations of state. Fig. 8 is a generalization of Fig. 10 of Ref. [16], showing the effect of different nuclear matter EoSs and different transition densities.

We see that, as expected from Fig. 3, hybrid stars will be heavier if the energy density discontinuity $\Delta\epsilon$ is smaller (so the gravitational pull of the core does not destabilize the star) and the speed of sound in quark matter is higher (so the core is stiffer and can support a

heavy star).

For the softer HLPS EoS, whose pure nuclear matter star has a maximum mass of $2.15 M_\odot$ (Table I), hybrid stars can be heavier than the pure nuclear star. This occurs when the transition density is low, and the quark core is a large fraction of the star. In the $M(R)$ relation, the hybrid branch can have a positive dM/dR , so its $M(R)$ curve looks similar to that of a pure quark matter star, rising to a maximum mass star which is heavier and larger than the heaviest pure HLPS star. For the harder NL3 EoS, whose pure nuclear matter star has a maximum mass of $2.77 M_\odot$, hybrid stars are always lighter than the heaviest nuclear matter star.

C. The quark matter mass fraction

For hybrid stars, it is natural to ask how much of the mass of the star consists of quark matter. We define the quark matter mass fraction $f_q \equiv M_{\text{core}}/M_{\text{star}}$. In Fig. 8(a), along the thick (blue, $n_{\text{trans}} = 4n_0$) contours of constant M_{star} , f_q varies from about 60% at low c_{QM}^2 and $\Delta\epsilon$ to about 70% at high c_{QM}^2 and $\Delta\epsilon$. If the transition pressure is lower then we expect the quark fraction to be larger: along the medium-thickness (green) mass contours for $n_{\text{trans}} = 2n_0$, f_q varies from about 90% at low c_{QM}^2 and $\Delta\epsilon$ to about 96% at high c_{QM}^2 and $\Delta\epsilon$.

In Fig. 8(b), along the medium-thickness (green) mass contours for $n_{\text{trans}} = 2n_0$, f_q varies from about 50% at low c_{QM}^2 and $\Delta\epsilon$ to about 80% at high c_{QM}^2 and $\Delta\epsilon$. Again, if the transition pressure is lower then the quark fraction is larger: along the thin (red) mass contours for $n_{\text{trans}} = 1.5n_0$, f_q varies from about 80% at low c_{QM}^2 and $\Delta\epsilon$ to over 90% at high c_{QM}^2 and $\Delta\epsilon$.

V. CONCLUSIONS

We studied hybrid stars where there is a sharp interface between two phases with different equations of state. We called the two phases “nuclear matter” and “quark matter”, but our conclusions are valid for any first-order phase transition between two phases with different energy densities.

It is already known that in the presence of such a first-order phase boundary there will be a stable connected branch of hybrid stars if the energy density discontinuity $\Delta\epsilon$ at the transition is less than a critical value $\Delta\epsilon_{\text{crit}}$ (Eq. (2)) which depends only on the ratio of pressure to nuclear matter energy density at the transition. We confirmed this result and investigated the conditions for the occurrence of a disconnected hybrid branch, and the visibility of the hybrid branches. To study these properties of hybrid stars we used a fairly generic Classical Ideal Gas (CIG) parameterization of the quark matter EoS at densities beyond the transition, and came to the following conclusions.

(1) Even if there is no connected hybrid star branch, there may be a disconnected one if the transition density is low enough and the speed of sound is high enough so that the nuclear mantle can be supported by a large enough quark matter core, and the energy density discontinuity is large enough so that a medium-sized core has insufficient pressure to support the nuclear mantle (see Fig. 3).

(2) The phase diagram for disconnected hybrid star branches is largely determined by the parameters of the QM EoS, $p_{\text{trans}}/\epsilon_{\text{trans}}$, $\Delta\epsilon/\epsilon_{\text{trans}}$, and c_{QM}^2 . It is not very sensitive to the detailed form of the nuclear matter EoS.

(3) Even if, according to the standard criterion (2), a connected hybrid branch is present, it may be so short as to be very hard to detect by measurements of the mass and radius of the star (see Fig. 5). When a disconnected branch is present, the connected branch is either absent or very small.

(4) We confirmed that the relationship (3) between the maximum mass of a star and its central energy density, which was proposed in Ref. [30], holds for hybrid stars (see Fig. 7).

(5) We found that it is possible to get heavy hybrid stars (more than $2 M_\odot$) for reasonable parameters of the quark matter EoS. It requires a not-too-high transition density ($n_{\text{trans}} \sim 2n_0$), low enough energy density discontinuity $\Delta\epsilon \lesssim 0.5\epsilon_{\text{trans}}$, and high enough speed of sound $c_{\text{QM}}^2 \gtrsim 0.4$. It is interesting to note that free quark matter would have $c_{\text{QM}}^2 = 1/3$, and a value of c_{QM}^2 that is well above $1/3$ is an indication that the quark matter is strongly coupled. For a stiff nuclear matter EoS such as NL3 it was somewhat easier to make heavy hybrid stars. Details are presented in Fig. 8. Our findings provide a generic formulation of the results found in previous calculations for specific models of quark matter, e.g., [12, 19], which found that in the absence of theoretical or experimental constraints on the quark matter EoS, one can fairly easily vary the unknown parameters of that EoS to obtain heavy hybrid stars. For now, it seems clear that without theoretical advances that constrain the form of the quark matter EoS, measurements of gross features of the $M(R)$ curve such as the maximum mass will not be able to rule out the presence of quark matter in neutron stars.

Our overarching message is that the generic CIG parameterization of the quark matter EoS (also used in Ref. [16]) provides a general framework for comparison and empirical testing of models of the quark matter EoS. Any particular model can be characterized, at least at densities that are not too far from the transition, in terms of its values of the parameters $p_{\text{trans}}/\epsilon_{\text{trans}}$, $\Delta\epsilon/\epsilon_{\text{trans}}$, and c_{QM}^2 , and its predictions for hybrid stars will follow from these values, which determine its position in the phase diagram (Fig. 3). If the form of the nuclear matter EoS were established then measurements of the $M(R)$ relation of neutron stars could be directly expressed as constraints on the values of our quark matter EoS parameters.

The CIG parameterization relies on the assumption of

a density-independent speed of sound, which is a useful starting point for general comparisons between quark matter models, as well as providing specific examples of quark matter equations of state that can yield heavy hybrid stars (Fig. 8). If observations of $M(R)$ for heavy stars turned out to be inconsistent with this parameterization, or if theorists were able to show that the speed of sound in quark matter has significant density dependence, then this approach could be further generalized (at the penalty of introducing more parameters) to allow for that, and to allow for mixed or percolated phases as noted in Refs. [11, 12].

Acknowledgments

We thank David Blaschke and Pavel Haensel for pointing out relevant earlier work. This research was supported in part by the Offices of Nuclear Physics and High Energy Physics of the Office of Science of the U.S. Department of Energy under contracts #DE-FG02-91ER40628 (for M.G.A.), #DE-FG02-05ER41375 (for M.G.A. and S.H.), #DE-FG02-93ER-40756 (for M.P.), and by the DOE Topical Collaboration “Neutrinos and Nucleosynthesis in Hot and Dense Matter”, contract #DE-SC0004955.

Appendix A: Classical Ideal Gas equation of state

Here we briefly recapitulate (see, e.g., Ref. [16]) the construction of a thermodynamically consistent equation of state of the form in Eq. (1)

$$\varepsilon(p) = \varepsilon_0 + \frac{1}{c^2} p. \quad (\text{A1})$$

We start by writing the pressure in terms of the chemical potential

$$\begin{aligned} p(\mu_B) &= A \mu_B^{1+\beta} - B, \\ \mu_B(p) &= \left(\frac{p+B}{A} \right)^{1/(1+\beta)}. \end{aligned} \quad (\text{A2})$$

Note that we have introduced an additional parameter A with mass dimension $3 - \beta$. The value of A can be varied without affecting the energy-pressure relation (A1). When constructing a first-order transition from some low-pressure EoS to a high-pressure EoS of the form (A1), we must choose A so that the pressure is a monotonically increasing function of μ_B (i.e. so that the jump in n_B at the transition is not negative). The derivative with respect to μ_B yields

$$n_B(\mu_B) = (1 + \beta) A \mu_B^\beta \quad (\text{A3})$$

and using $p = \mu_B n_B - \varepsilon$, we obtain the energy density

$$\varepsilon(\mu_B) = B + \beta A \mu_B^{1+\beta}. \quad (\text{A4})$$

Then Eq. (A2) gives energy density as a function of pressure

$$\varepsilon(p) = (1 + \beta) B + \beta p \quad (\text{A5})$$

which is equivalent to Eq. (A1) with $1/c^2 = \beta$ and $\varepsilon_0 = (1 + \beta) B$.

-
- [1] A. Akmal, V. Pandharipande, and D. Ravenhall, *The Equation of state of nucleon matter and neutron star structure*, Phys.Rev. **C58** (1998) 1804–1828, [[nucl-th/9804027](#)].
 - [2] K. Hebeler, J. Lattimer, C. Pethick, and A. Schwenk, *Constraints on neutron star radii based on chiral effective field theory interactions*, Phys.Rev.Lett. **105** (2010) 161102, [[arXiv:1007.1746](#)].
 - [3] S. Gandolfi, J. Carlson, and S. Reddy, *The maximum mass and radius of neutron stars and the nuclear symmetry energy*, Phys.Rev. **C85** (2012) 032801, [[arXiv:1101.1921](#)].
 - [4] I. M. Barbour, S. E. Morrison, E. G. Klepfish, J. B. Kogut, and M.-P. Lombardo, *Results on finite density QCD*, Nucl. Phys. Proc. Suppl. **60A** (1998) 220–234, [[hep-lat/9705042](#)].
 - [5] M. G. Alford, A. Kapustin, and F. Wilczek, *Imaginary chemical potential and finite fermion density on the lattice*, Phys. Rev. **D59** (1999) 054502, [[hep-lat/9807039](#)].
 - [6] J. Cox, C. Gatttringer, K. Holland, B. Scarlet, and U. J. Wiese, *Meron-cluster solution of fermion and other sign problems*, Nucl. Phys. Proc. Suppl. **83** (2000) 777–791, [[hep-lat/9909119](#)].
 - [7] S. Hands, *Simulating dense matter*, Prog. Theor. Phys. Suppl. **168** (2007) 253–260, [[hep-lat/0703017](#)].
 - [8] M. G. Alford, K. Rajagopal, S. Reddy, and F. Wilczek, *The Minimal CFL nuclear interface*, Phys.Rev. **D64** (2001) 074017, [[hep-ph/0105009](#)].
 - [9] L. F. Palhares and E. S. Fraga, *Droplets in the cold and dense linear sigma model with quarks*, Phys.Rev. **D82** (2010) 125018, [[arXiv:1006.2357](#)].
 - [10] M. B. Pinto, V. Koch, and J. Randrup, *The Surface Tension of Quark Matter in a Geometrical Approach*, [arXiv:1207.5186](#).
 - [11] J. Macher and J. Schaffner-Bielich, *Phase transitions in compact stars*, Eur.J.Phys. **26** (2005) 341–360, [[astro-ph/0411295](#)].
 - [12] K. Masuda, T. Hatsuda, and T. Takatsuka, *Hadron-Quark Crossover and Massive Hybrid Stars*, [arXiv:1212.6803](#).
 - [13] Z. F. Seidov, *The Stability of a Star with a Phase Change in General Relativity Theory*, Sov. Astron. **15** (Oct.),

- 1971) 347.
- [14] R. Schaeffer, L. Zdunik, and P. Haensel, *Phase transitions in stellar cores. I - Equilibrium configurations*, Astron. Astrophys. **126** (Sept., 1983) 121–145.
 - [15] L. Lindblom, *Phase transitions and the mass radius curves of relativistic stars*, Phys.Rev. **D58** (1998) 024008, [gr-qc/9802072].
 - [16] J. Zdunik and P. Haensel, *Maximum mass of neutron stars and strange neutron-star cores*, arXiv:1211.1231.
 - [17] A. Kurkela, P. Romatschke, A. Vuorinen, and B. Wu, *Looking inside neutron stars: Microscopic calculations confront observations*, arXiv:1006.4062.
 - [18] A. Kurkela, P. Romatschke, and A. Vuorinen, *Cold Quark Matter*, Phys.Rev. **D81** (2010) 105021, [arXiv:0912.1856].
 - [19] M. Alford, M. Braby, M. Paris, and S. Reddy, *Hybrid stars that masquerade as neutron stars*, Astrophys.J. **629** (2005) 969–978, [nucl-th/0411016].
 - [20] G. Shen, C. Horowitz, and S. Teige, *A New Equation of State for Astrophysical Simulations*, Phys.Rev. **C83** (2011) 035802, [arXiv:1101.3715].
 - [21] J. M. Lattimer and Y. Lim, *Constraining the Symmetry Parameters of the Nuclear Interaction*, arXiv:1203.4286.
 - [22] A. W. Steiner, J. M. Lattimer, and E. F. Brown, *The Equation of State from Observed Masses and Radii of Neutron Stars*, Astrophys. J. **722** (2010), no. 1 33, [arXiv:1005.0811].
 - [23] J. M. Bardeen, K. S. Thorne, and D. W. Meltzer, *A catalogue of methods for studying the normal modes of radial pulsation of general-relativistic stellar models*, Astrophys. J. **145** (Aug., 1966) 505–+.
 - [24] J. L. Zdunik, P. Haensel, and R. Schaeffer, *Phase transitions in stellar cores. II - Equilibrium configurations in general relativity*, Astron. Astrophys. **172** (Jan., 1987) 95–110.
 - [25] N. K. Glendenning and C. Kettner, *Possible third family of compact stars more dense than neutron stars*, Astron. Astrophys. **L9** (2000) 353.
 - [26] K. Schertler, C. Greiner, J. Schaffner-Bielich, and T. M. H., *Quark phases in neutron stars and a "third family" of compact stars as a signature for phase transitions*, Nucl. Phys. **A677** (2000) 463, [astro-ph/0001467].
 - [27] V. Thorsson, M. Prakash, and J. M. Lattimer, *Composition, Structure, and Evolution of Neutron Stars with Kaon Condensates*, Nucl. Phys. **A572** (1994) 693.
 - [28] E. S. Fraga, R. D. Pisarski, and J. Schaffner-Bielich, *Small, dense quark stars from perturbative QCD*, Phys. Rev. **D63** (2001) 121702, [hep-ph/0101143].
 - [29] S. Banik and D. Bandyopadhyay, *Color superconducting quark matter core in the third family of compact stars*, Phys. Rev. **D67** (2003) 123003.
 - [30] J. M. Lattimer and M. Prakash, *What a Two Solar Mass Neutron Star Really Means*, in *From Nuclei To Stars: Festschrift in Honor of Gerald E Brown* (S. Lee, ed.), pp. 275–304. World Scientific, 2011. arXiv:1012.3208.
 - [31] I. Mishustin, M. Hanauske, A. Bhattacharyya, L. Satarov, H. Stoecker, et. al., *Catastrophic rearrangement of a compact star due to the quark core formation*, Phys.Lett. **B552** (2003) 1–8, [hep-ph/0210422].
 - [32] L.-M. Lin, K. Cheng, M.-C. Chu, and W.-M. Suen, *Gravitational waves from phase-transition induced collapse of neutron stars*, Astrophys.J. **639** (2006) 382–396, [astro-ph/0509447].
 - [33] J. M. Lattimer and M. Prakash, *The Ultimate energy density of observable cold matter*, Phys.Rev.Lett. **94** (2005) 111101, [astro-ph/0411280].
 - [34] P. Demorest, T. Pennucci, S. Ransom, M. Roberts, and J. Hessels, *Shapiro Delay Measurement of A Two Solar Mass Neutron Star*, Nature **467** (2010) 1081–1083, [arXiv:1010.5788].
 - [35] J. Antoniadis, P. C. Freire, N. Wex, T. M. Tauris, R. S. Lynch, et. al., *A Massive Pulsar in a Compact Relativistic Binary*, Science **340** (2013) 6131, [arXiv:1304.6875].
 - [36] For a classical ideal gas, the squared speed of sound $c_s^2 \propto T/m$, where T is the temperature and m is the mass, and is independent of density. For a quantum ideal gas, $c_s^2 = (1/3) (1 - (m/\mu)^2)$, where μ is the chemical potential inclusive of mass, and varies between 1/3 (ultra-relativistic case) and $\sim (2/3) n^{2/3}$ (the non-relativistic case), where n is the number density.